Published in final edited form as:
*J Trauma*. 2011 July ; 71(1 Suppl): S151–S160. doi:10.1097/TA.0b013e318221aa4c.

# Decay-Accelerating Factor Mitigates Controlled Hemorrhage-Instigated Intestinal and Lung Tissue Damage and Hyperkalemia in Swine

**Jurandir J. Dalle Lucca, PhD**[1], **Milomir Simovic, PhD**[1], **Yansong Li, MD**[1], **Chantal Moratz, PhD**[2], **Michael Falabella, BS**[1], and **George C. Tsokos, MD**[3]

Milomir Simovic: Milomar.simovic@amedd.army.mil; Yansong Li: Yansong.li@amedd.army.mil; Chantal Moratz: Cmoratz@usuhs.mil; Michael Falabella: Michael.Falabella@amedd.army.mil; George C. Tsokos: gtsokos@bidmc.harvard.edu

[1]ImmunoModulation of Trauma Program, United States Army Institute of Surgical Research, 3650 Chambers Pass, Fort Sam Houston, TX 78234-6315

[2]Department of Medicine, Uniformed Services University for the Health Sciences Bethesda, MD 20814

[3]Department of Medicine, Beth Israel Deaconess Medical Center, Harvard Medical School, Boston, MA 02215

## Abstract

**Background—**Activation of complement system has been associated with tissue injury after hemorrhage and resuscitation in rats and swine. This study investigated whether administration of human recombinant decay-accelerating factor (DAF; a complement regulatory protein that inhibits classical and alternative pathways) reduces tissue damage in a porcine model of hemorrhagic shock.

**Methods—**Male Yorkshire swine assigned to four groups were subjected to controlled, isobaric hemorrhage over 15 minutes to a target mean arterial pressure of 35 mmHg. Hypotension was maintained for 20 minutes followed by a bolus intravenous injection of DAF or vehicle then animals were observed for 200 minutes. Blood chemistry and physiological parameters were recorded. Tissue samples from lung and small intestine were subjected to histopathological evaluation and detection of tissue deposition of complement proteins by immunohistochemistry and Western blot analyses.

**Results—**Administration of DAF significantly reduced intestinal and lung tissue damage in a dose-dependent manner (5, 25, and 50 μg/kg). In addition, DAF treatment improved hemorrhage-induced hyperkalemia. The protective effects of DAF appear to be related to its ability to reduce tissue complement activation and deposition on affected tissues.

**Conclusions—**DAF treatment decreased tissue complement activation and deposition in hemorrhaged animals and attenuated tissue damage at 200 minutes post treatment. The observed

Corresponding author: Jurandir.dallelucca@us.army.mil, US Army Institute of Surgical Research, 3400 Rawley E. Chambers Ave., Fort Sam Houston, TX 78234, (210) 916-3698, Fax (210) 916-9291.

# Report Documentation Page

*Form Approved*
*OMB No. 0704-0188*



| 1. REPORT DATE | 2. REPORT TYPE | 3. DATES COVERED |
|---|---|---|
| **01 JUL 2011** | **N/A** | **-** |

| 4. TITLE AND SUBTITLE | 5a. CONTRACT NUMBER |
|---|---|
| **Decay-accelerating factor mitigates controlled hemorrhage-instigated intestinal and lung tissue damage and hyperkalemia in swine** | 5b. GRANT NUMBER |
| | 5c. PROGRAM ELEMENT NUMBER |
| 6. AUTHOR(S) | 5d. PROJECT NUMBER |
| **Dalle Lucca J. J., Simovic M., Li Y., Moratz C., Falabella M., Tsokos G. C.,** | 5e. TASK NUMBER |
| | 5f. WORK UNIT NUMBER |
| 7. PERFORMING ORGANIZATION NAME(S) AND ADDRESS(ES) | 8. PERFORMING ORGANIZATION REPORT NUMBER |
| **United States Army Institute of Surgical Research, JBSA Fort Sam Houston, TX** | |
| 9. SPONSORING/MONITORING AGENCY NAME(S) AND ADDRESS(ES) | 10. SPONSOR/MONITOR'S ACRONYM(S) |
| | 11. SPONSOR/MONITOR'S REPORT NUMBER(S) |

12. DISTRIBUTION/AVAILABILITY STATEMENT
**Approved for public release, distribution unlimited**

13. SUPPLEMENTARY NOTES

14. ABSTRACT

15. SUBJECT TERMS

| 16. SECURITY CLASSIFICATION OF: | | | 17. LIMITATION OF ABSTRACT | 18. NUMBER OF PAGES | 19a. NAME OF RESPONSIBLE PERSON |
|---|---|---|---|---|---|
| a. REPORT | b. ABSTRACT | c. THIS PAGE | | | |
| **unclassified** | **unclassified** | **unclassified** | **UU** | **20** | |

beneficial effects of DAF treatment on tissue injury after 20 minutes of severe hypotension presents an attractive model of small volume resuscitation, particularly in situations with a restrictive medical logistical footprint such as far-forward access to first responders in the battlefield or in remote rural or mountainous environments.

### Keywords

ischemia; resuscitation; complement system; decay accelerating factor; hemorrhage

## Introduction

A significant portion of hemorrhage-related mortality has been attributed to delays in hemorrhage control during transportation or resuscitation.[1] A substantial number of trauma victims who survive the initial hemorrhage subsequently succumb to complications resulting from systemic inflammatory response in the form of multiple organ dysfunction syndrome (MODS)[2] or acute respiratory distress syndrome (ARDS),[3] which occur despite seemingly acceptable medical therapy and surgical intervention.[4]

The first physiologic response to severe blood loss is activation of the neuroendocrine response leading to vasoconstriction. This attempts to shift blood away from the bleeding site towards more vital organs, such as the heart, lungs, and brain, also drives blood away from the intestines which leads to functional intestinal ischemia.[5] Intestinal ischemia leads to systemic inflammatory response rendering the body particularly susceptible to inflammatory complications following hemorrhage.[4]

Late morbidity and mortality following hemorrhage results from the involvement of multiple inflammatory pathways, including complement. Excessive complement activation has been implicated in the pathogenesis of ischemia/reperfusion-induced intestinal damage and inflammation[6] and hemorrhagic shock.[2] We and others have reported that complement activation is critical for ischemia/reperfusion induced intestinal injury[6] and hemorrhage-induced inflammation and intestinal damage in mice.[7] Both local and systemic complement activation[8] are part of a common inflammatory cascade in the pathogenesis of tissue damage and organ dysfunction in the early phase after trauma.[9] Complement activation in patients occurs immediately after trauma and its activity relates to the severity of the injury and associated complications.[10]

Maintenance of tissue oxygenation with adequate fluid resuscitation is believed to be critical in the management of hemorrhagic patients. However, even the most effective resuscitation strategies remain controversial. Conventional resuscitation strategies, such as intravenous administration of crystalloids and colloids can exacerbate cellular injury caused by hemorrhagic shock.[11] Therefore, strategies aimed at reducing or even eliminating the need for resuscitation fluid infusion have been identified as a major requirement.[11,12]

Complement inhibition has been shown to be an attractive therapeutic strategy in intestinal ischemia/reperfusion in mice[6,13] as well as in rats for traumatic and hemorrhagic shock.[14] In this study, we demonstrate that infusion of DAF in swine after 20 minutes of severe hypotension mitigated gut and lung injury and reduced hyperkalemia. We propose that DAF infusion may represent a modality of pharmacologic resuscitation or adjunct to small volume fluid resuscitation.

## Materials and Methods

After Institutional Animal Care and Use Committee approval, immature male swine underwent controlled isobaric arterial hemorrhage with target mean arterial pressure (MAP) of 35 mmHg for 20 minutes followed by 60 ml bolus of DAF or vehicle (Phosphate Buffered Saline, PBS). This study was conducted in compliance with the Animal Welfare Act, the Implementing Animal Welfare Regulations and in accordance with the principles of the Guide for the Care and Use of Laboratory Animals.

### Animal preparation and physiologic monitoring

Immature, castrated male Yorkshire crossbred swine (12 weeks old, 30–38 kg, Sus scrofa; ABI, Danboro, PA) were fasted overnight with free access to water. The swine were anesthetized (Ketamine, 20mg/kg b.w. and Xylazine, 2.2mg/kg b.w. intramuscular injection) then underwent surgical placement of pre-hirudinized (100μg of Refludan®/ml saline; ZLB Behring GmbH, Marburg, Germany) catheters (Starflex, 9Fr, 11 cm; Inver Grove Heights, MN) under sterile conditions into the left femoral artery and vein under isoflurane anesthesia (3% induction, 2–2.6% maintenance; Minrad, Buffalo, NY). Immediately after placement and periodically after blood sampling, the catheters were flushed with 2 ml of hirudinized saline to ensure patency. Hemorrhage and withdrawal of blood samples were performed via the artery. Sixty ml of PBS containing various doses of DAF or 60 ml PBS was administered into the vein. A micromanometer (MPC-500; Millar Instruments, Houston, TX) was inserted into the right femoral artery for hemodynamic monitoring by Computer Assisted Resuscitation Algorithm (CARA) software.

### Experimental design

The animals were hemorrhaged using a controlled, isobaric Wiggers model of controlled hemorrhagic shock (Figure 1). The animals were randomly enrolled in one of five experimental groups: 1) Control, sham operated (cannulated but not hemorrhaged, n = 5); 2) H, hemorrhage + vehicle (60ml PBS, n = 6); 3) H + D5, hemorrhage + 5μg/kg b.w. DAF (n = 6); 4) H + D25, hemorrhage + 25μg/kg b.w. DAF (n = 6); and 5) H + D50, hemorrhage + 50μg/kg b.w. DAF (n = 8).

The doses of DAF used in this study were chosen based on our investigations of ischemia-reperfusion in mice and hemorrhagic shock in rats.[6,13] A dose of DAF (60μg/kg b.w., iv) had beneficial effects in hemorrhaged rats. For this study, the doses of DAF were titrated upward at intervals until the optimal beneficial effect was achieved.

The animals were spontaneously ventilated. Anesthesia was maintained with 2% isoflurane in 99% oxygen before and during surgical dissection of the blood vessels. Upon surgery anesthesia was maintained with 2% isoflurane while the animals spontaneously ventilated oxygen/nitrogen (22%/78%) through a semi-closed loop system. Controlled arterial hemorrhage was automated to insure reproducibility. In brief, a customized computer protocol (LabView v. 8.2; National Instruments, Austin, TX) monitored MAP. Using a proportional control feedback algorithm, the program controlled the speed and direction of a partial occlusion roller pump (Masterflex Digital Console Drive; Cole-Parmer Instruments, Chicago, IL) that was connected to the femoral arterial catheter. At the start of the hemorrhage phase, the computer started withdrawing blood to decrease MAP to the target pressure over a 15 minute period. During the protocol, the volume of withdrawn blood was gravimetrically measured (PB5001-S; Mettler-Toledo, Columbus, OH) and the data output was stored on computer hard disk with time stamped hemodynamic parameters. Twenty minutes after MAP reached 35 mm Hg, a bolus of recombinant human DAF in PBS (60 ml) was administered. The animals were then monitored for 200 minutes.

As indicated in figure 1, a total of 16 arterial blood samples were obtained: prior to surgery (−60 min), prior to hemorrhage (−15 and −5 min prehemorrhage), hemorrhage to MAP of 35 mmHg (5 and 15 min postshock), immediately before DAF administration (35 min, postshock), then at 20 minute intervals until the end of the observation period (235 min). Blood samples were analyzed for pH, $pCO_2$, $pO_2^-$, bicarbonate ($HCO_3^-$), base excess (BE), lactate, glucose, hematocrit (Hct), hemoglobin (Hb), sodium ($Na^+$), potassium ($K^+$), and ionized calcium ($iCa^{2+}$) using i-STAT cartridges (Abbott Laboratories, Abbott Park, IL).

### Tissue harvest

The animals were euthanatized with isoflurane at the endpoint following the aforementioned procedures. Tissue samples, including lung and intestine were removed, frozen on dry-ice and either stored at −80°C for determining protein expression or fixed with 10% formalin or 4% paraformaldehyde for histological and immunohistochemical analysis.

### Tissue protein extraction

Frozen tissue samples were thawed, washed with ice-cold PBS, suspended in radio-immunoprecipitation assay (RIPA) buffer containing protease inhibitors [2μg/ml of aprotinin, 10μM of leupeptin, 1mM of phenylmethylsulfonyl fluoride (PMSF)] and minced on ice. The samples were sonicated on ice using a sonicator (Ultrasonics Co., Danbury, CT) at setting 5 for 4×10s at continuous output with 10s pauses between the cycles. The samples were then centrifuged at 13,000 rpm for 10min at 4°C. The supernatants were frozen and stored at −80°C until assayed for C3a and C5b-9. Aliquots were used to determine protein concentration by Bio-Rad protein assay (Bio-Rad Laboratories, CA).

### Reagents and antibodies

All antibodies were validated to work in swine. Recombinant human DAF/CD55 was obtained from R&D Systems (Minneapolis, MN). CG4+ and CG8+ cartridges were purchased from Abbott (Princeton, NJ). Chicken anti-C3/C3a, mouse anti-C5/C5a, mouse anti-C5b-9, and mouse anti-endothelial cell (EC) antibodies were obtained from Abcam Inc. (Cambridge, MA). Glyceraldehyde 3-phosphate dehydrogenase (GAPDH) was from Sigma-Aldrich (St. Louis, MO). Goat anti-chicken Alexa Fluor 594, goat anti-mouse Alexa Fluor 488, goat anti-mouse Alexa Fluor 594 IgG (H+L) conjugated secondary antibodies, and ProLong Gold antifade reagent were from Invitrogen (Carlsbad, CA).

### Western-blotting

Tissue extracts were separated by electrophoresis on sodium dodecyl sulfate polyacrylamide gel electrophoresis (SDS-PAGE) and transferred onto a polyvinylidene difluoride membrane. The membranes were blocked with 5% nonfat dry milk in Tris-buffered saline with Tween-20 (TBST) for 1 hour then incubated with primary antibodies, anti-C3a and GAPDH (control), for 1 hour followed by incubation with appropriate horseradish peroxidase (HRP)-conjugated secondary antibodies for 1 hour. Specific bands were visualized by the Enhanced Chemiluminescence (ECL) method (Amersham Biosciences, Piscataway, NJ) and captured with Fujifilm LAS-3000 System Configured for Chemiluminescence (Fujifilm Life Science, Edison, NJ). The density of each band was measured using QuantityOne Software (BioRad, Hercules, NJ).

### Dot-blotting

For efficient transfer of proteins onto nitrocellulose membrane, Dot Blot 96 System (Labrepco Inc., Horsham, PA) was utilized. Briefly, 200 μl of sample containing 1 μg protein was loaded into each well using multichannel pipettors then the sample was vacuumed with a vacuum pump. After the membrane dried, it was blocked with 5% nonfat

dry milk in TBST for 1 hour at room temperature, incubated with primary antibodies (C5b-9 or GAPDH) for 1 hour followed by incubation with appropriate HRP-conjugated secondary antibodies for 1 hour at room temperature. Specific bands were visualized by the ECL method (Amersham Biosciences, Piscataway, NJ) and captured with Fujifilm LAS-3000 System Configured for Chemiluminescence (Fujifilm Life Science, Edison, NJ). The density of each band was measured using QuantityOne Software (BioRad, Hercules, NJ).

### Histological examination

10% formalin-fixed tissues were embedded in paraffin, sectioned, and stained with hematoxylin-eosin (H&E). Histological images were recorded under a light microscope (Olympus AX80, Center Valley, PA) with 10× objective by a pathologist blind to the treatment group. Histological injury scores were graded using the following scale:

- For lung injury, four parameters (alveolar fibrin edema, alveolar hemorrhage, septal thickening, and intra-alveolar inflammatory cells) were scored on each H&E stained slide for: 1) severity (0: absent; 1, 2, and 3 for more severe changes) and 2) extent of injury (0: absent; 1: <25%; 2: 25–50%; 3: >50%). Total injury score for each slide was calculated as the sum of the extent plus the severity of injury.
- Mucosal damage of small intestine for each slide was graded on a six-tiered scale: 0 for normal villus; 1 for villi with tip distortion; 2 for villi lacking goblet cells and containing Guggenheims' spaces; 3 for villi with patch disruption of the epithelial cells: 4 for villi with exposed but intact lamina propria and epithelial cell sloughing; 5 for villi in which the lamina propria was exuding; and 6 for hemorrhaged or denuded villi.

### Immunohistochemical staining

Paraformaldehyde-fixed lung and small intestine biopsies were snap-frozen at −70°C, sections were cut at a 5μm-thickness with a cryostat and fixed in cold methanol for 20 minutes. The fixed sections were permeabilized with 0.2% Triton X-100 in PBS for 10 minutes and blocked with 2% BSA in PBS for 30 minutes at room temperature. The sections were incubated with the primary antibodies (C5b-9, C5, or C3) overnight at 4°C, washed, then incubated with the appropriate secondary antibodies labeled with Alexa Fluor 488 and 594 for 1 hour at room temperature. After washing, the sections were mounted with ProLong Gold antifade solution containing 4', 6'-diamidino-2-phenylindole (DAPI, a fluorescent stain that binds strongly to DNA) and visualized under a confocal laser scanning microscope (Radiance 2100; Bio-Rad, Hercules, NJ) at 400× magnification. Captured digital images were processed by Image J software (NIH, Bethesda, MD).

### Immunofluorescent quantification of complement factors

This procedure was based on a modified method as previous described.[13] Briefly, four to six immunohistochemical slides from the lung and small intestine were imaged from each animal and were opened using Adobe Photoshop software then adjusted until only the fluorescent deposits and no background tissue were visible. Using Image J software, the image was changed to black and white pixels with black representing deposits of the target proteins and white representing nonstained areas of the image. Using the image Adjust Threshold command, the image was then changed to red and white, fluorescent deposits being red. The image was analyzed to result in the total red area in pixels squared. Values for total area for all animals in each group were averaged to give the average area of fluorescent deposit.

### Statistical analysis

Data are expressed as mean ± SEM. One- or two-way ANOVA followed by Bonferonni or Tukey's post-test was performed using GraphPad Prism (4.0, GraphPad Software, San Diego, CA). *P* value <0.05 was considered as significant.

## Results

In order to investigate the direct effects of DAF on hemorrhagic shock, animals were subjected to controlled bleeding to a MAP target fixed at 35 mmHg for 20 minutes followed by bolus i.v. injection of DAF (5, 25, or 50 μg/kg b.w.) as outlined in figure 1. This procedure is not lethal during the 200 minute post-hemorrhage observation period, therefore the primary endpoint for this set of experiments was the histopathological analysis of lungs and gut. Deposition of complement proteins in lungs and gut tissues collected at the end of experiment was also determined. Secondary endpoints included physiologic and blood metabolic analysis throughout the course of experiment.

### Baseline characteristics

No differences were observed in weight, Hb, Hct, arterial pH, $pO_2$, $sO_2$, $pCO_2$, $HCO_3$-, BE, glucose, lactate, $K^+$, $Na^+$, MAP, shock index (SI), or pulse pressure (PP) during the baseline phase of pre-hemorrhage among sham, control, and DAF treated groups (Tables 1 and 2). Compared to the Sham group, $iCa^{2+}$ at the pre-hemorrhage time was significantly higher in the H+D5 and H+D25 groups and remained so throughout the experiment (Table 2). At the postshock phase, the only parameters which showed significant differences were BE, $HCO_3^-$ and glucose (Table 2).

### Effects of DAF on metabolic and hemodynamic parameters

At the end of postshock phase, $K^+$ levels from hemorrhaged control animals were significantly elevated when compared to Sham group whereas $K^+$ levels were lower after infusion of a high dose of DAF (50 μg/kg) when compared to hemorrhaged control animals at the end of experiment (Table 2). At the end of observation period, serum lactate was found to be significantly elevated in controlled hemorrhaged animals when compared to sham group, however DAF treatment did not significantly affect lactate concentration compared with H group. MAP and PP decreased while SI increased in the hemorrhaged animals compared to the Sham group at the end of hemorrhage phase (Table 1). There were no generalized changes in other metabolic parameters in the hemorrhaged animals in response to DAF treatment.

### Effect of DAF on hemorrhage induced intestinal damage

Intestinal tissue from hemorrhaged animals displayed obvious damage (Figure 2) with loss of mucosal villi in most areas accompanied by massive inflammatory cell infiltration, necrosis, moderate edema in the mucosa, and submucosa layers. Furthermore, the crypts were severely damaged. Intestinal tissue damage was found to be significantly decreased in hemorrhaged animals treated with 50μg/kg DAF, tissue damage remained superficial and villi were well preserved.

### Effect of DAF on complement activation and deposition in the small intestine tissue

Intravenous injection of DAF at a dose of 25 or 50μg/kg at the end of postshock phase led to a significant attenuation of hemorrhage-induced C5 deposition (Fig. 3A). C5b-9 formation was also inhibited by DAF in a dose-dependent manner similar to that of C5. Inhibition of C5b-9 by DAF was observed at a dose of 25 or 50μg/kg (Fig. 3B).

### Effect of DAF on hemorrhage-induced lung injury

H&E stained histological images and injury score (Figure 4) showed that pigs subjected to hemorrhagic shock displayed lung injury characterized by destruction of the alveolar architecture with severe alveolar hemorrhage, septal edema, and moderate inflammation when compared to the Sham group. Treatment with lower doses of DAF (5 or 25μg/kg) did not show a significant beneficial effect on tissue injury. However, hemorrhage-induced lung damage was significantly less in the DAF 50μg/kg group compared to the hemorrhage group.

### Effect of DAF on complement activation and deposition in the lung tissue

Lung deposition of C3 (Figure 5A) and C5 (Figure 5B) in hemorrhaged animals subjected to DAF treatment (25 or 50μg/kg) was less when compared to hemorrhaged animals. High amounts of C3a was detected by Western-blot of H lung tissue while the high dose DAF (50 μg/kg) treatment appreciably attenuated C3a generation (Figure 5C). Figure 5D shows more deposition of C5b-9 in lung tissue of the H group when compared with that of Sham, whereas the hemorrhaged animals that received DAF exhibited a reduction of C5b-9 formation. The localization and distribution pattern of C5b-9 in the lung tissue was also examined. As shown in figure 5D, C5b-9 accumulated and co-localized at the vascular endothelium of lung tissue. Dot-blotting of lung tissue showed a pattern of C5b-9 formation similar to what was observed with immunohistochemistry (Figure 5E).

## Discussion

Hemorrhagic shock is second only to central nervous system injury as cause death in trauma patients.[15] Treatments are aimed at restoring intravascular volume and maintaining vital organ perfusion.[11] Complement activation has been implicated during hemorrhage shock in rats[14] and swine,[16] and it relates to morbidity and mortality of trauma patients due to severe inflammatory tissue destruction.[17] Previously we showed that complement inhibition decreased resuscitation fluid requirements in hemorrhagic shock in rats.[14] We also showed that DAF treatment attenuated C-reactive protein (CRP)-enhanced tissue damage in a murine mesenteric ischemia/reperfusion (I/R) model[6] and protected neurons from hypoxia-mediated injury in vitro.[18]

The present study was designed to investigate the effects of DAF on hemodynamic and metabolic parameters as well as tissue injury in a controlled swine hemorrhagic shock model. It demonstrated that: 1) high dose of DAF (50μg/kg) significantly attenuated hemorrhage associated lung and gut injury, complement deposition, and blood potassium levels; and 2) deposition and activation of complement at the tissue level was suppressed in tissue from animals who had received DAF.

A direct correlation has been shown between early complement activation (<30 min after trauma) and injury severity in patients,[17] furthermore, concentrations of C3a and C3a/C3 ratio in the blood plasma have been shown to relate directly to the clinical severity of trauma in patients.[19]

DAF decays C3/5 convertases of both the classical and alternative pathways and contains four extracellular short consensus repeat (SCR) domains linked to the membrane by a glycosylphosphatidylinositol (GPI) anchor.[20] In the present study we show that administration of a single dose of DAF after 20 minutes of severe hypotension resulted in a significant reduction of complement activation as manifested by lower deposition of complement products on gut and lung tissues. Decreased amounts of the anaphylatoxin C3a could account for the decreased inflammatory response and limited deposition of C5b-9 may account for the recorded mitigated tissue damage.

DAF has well defined complement regulatory functions,[18] additionally it has been claimed to interfere with cell signaling. DAF has been found to associate with Src protein tyrosine kinases such as p56lck and p59fyn in human T cells[21] and recently we showed that DAF suppresses the activation of c-Src in cultured neuronal cells subjected to ischemia-like conditions.[18] Although the mechanism by which DAF regulates activation of Src kinase is unknown, there is increasing evidence that Src family kinases act as a point of convergence for various signaling pathway, including the pathway that signals via G-coupled receptors. The inhibition of c-Src activity by DAF could be via a direct association of DAF and c-Src or indirectly via interruption of C3a-C3aR and/or C5a-C5aR signal pathways.[22] Thus, in addition to its complement modulatory actions, DAF may also prevent tissue damage by modifying cell signaling which may result in cell death.

Hyperkalemia is a medical emergency due to the risk of potentially fatal cardiac arrhythmia. Okamoto[23] showed that C5b-9 mediates changes of intracellular $Na^+$ and $K^+$ in rat skeletal muscle. Moreover, protein tyrosine kinase Src, MAPK, and reactive oxygen species (ROS) can modulate the activity of the Na+-K+-ATPase.[24] In our study hemorrhagic shock induced hyperkalemia was reduced by DAF (50 μg/kg). We hypothesize that the corrective role of DAF on hemorrhage induced hyperkalemia could result in protecting against hypoxic cellular damage by inhibiting C5b-9 formation and/or interruption of C5a-C5aR-Src/MAPK-$Na^+$-$K^+$-ATPase signal pathways. However, this assumption is speculative and needs further investigation.

The complement system has been considered as a functional bridge between the innate and adaptive immune systems allowing for the cross-talk between pattern recognition receptors such as C-reactive protein and Toll-like receptors.[25] We have recently reported that treatment with DAF inhibits C5a formation, IL-6 expression, accumulation of neutrophils, and release of myeloperoxidase (MPO) in both intestinal and lung tissue in mice subject to mesenteric I/R intensified by additional infusion of CRP.[6] It is possible therefore that the beneficial effects of DAF reported in the present study may relate to its broad ability to suppress inflammatory responses.

In conclusion, DAF treatment attenuated tissue damage and lowered tissue complement activation and deposition in hemorrhaged animals. Furthermore, the observed beneficial effects on tissue injury in DAF treated groups suggests an attractive alternative to standard fluid resuscitation, particularly in situations with a restrictive medical logistical footprint such as far-forward access to first responders in the battlefield or in remote rural or mountainous environments.

## Acknowledgments

The authors would like to acknowledge Shawn L. Dalle Lucca for editorial assistance. This study was funded by United States Army Medical Research and Materiel Command.

## References

1. Martin M, Oh J, Currier H, Tai N, et al. An analysis of in-hospital deaths at a modern combat support hospital. J Trauma. 2009; 66:S51–S60. [PubMed: 19359971]
2. Yao YM, Redl H, Bahrami S, et al. The inflammatory basis of trauma/shock-associated multiple organ failure. Inflamm Res. 1998; 47:201–210. [PubMed: 9657252]
3. Shoemaker WC, Appel P, Czer LS, et al. Pathogenesis of respiratory failure (ARDS) after hemorrhage and trauma: I. Cardiorespiratory patterns preceding the development of ARDS. Crit Care Med. 1980; 8:504–512. [PubMed: 7418426]
4. Cavaillon JM, Annane D. Compartmentalization of the inflammatory response in sepsis and SIRS. J Endotoxin Res. 2006; 12:151–170. [PubMed: 16719987]

5. Wenzel V, Raab H, Dünser MW. Arginine vasopressin: a promising rescue drug in the treatment of uncontrolled haemorrhagic shock. Best Pract Res Clin Anaesthesiol. 2008; 22:299–316. [PubMed: 18683476]
6. Lu X, Li Y, Simovic MO, et al. Decay-Accelerating Factor Attenuates C-Reactive Protein-Potentiated Tissue Injury After Mesenteric Ischemia/Reperfusion.
7. Fleming SD, Phillips LM, Lambris JD, et al. Complement component C5a mediates hemorrhage-induced intestinal damage. J Surg Res. 2008; 150:196–203. [PubMed: 18639891]
8. Li K, Sacks SH, Zhou W. The relative importance of local and systemic complement production in ischaemia, transplantation and other pathologies. Mol Immunol. 2007; 44:3866–3874. [PubMed: 17768105]
9. Ganter MT, Brohi K, Cohen MJ, et al. Role of the alternative pathway in the early complement activation following major trauma. Shock. 2007; 28:29–34. [PubMed: 17510601]
10. Tsukamoto T, Chanthaphavong RS, Pape HC. Current theories on the pathophysiology of multiple organ failure after trauma. Injury. 2010; 41:21–26. [PubMed: 19729158]
11. Pope, A.; French, G.; Longnecker, DE., editors. Fluid Resuscitation: State of the Science for Treating Combat Casualties and Civilian Injuries. Washington, D.C.: National Academy Press; 1999. p. 1-8.p. 47-78.p. 97-108.
12. Dubick MA, Atkins JL. Small-volume fluid resuscitation for the far-forward combat environment: current concepts. J Trauma. 2003; 54:S43–S45. [PubMed: 12768102]
13. Weeks C, Moratz C, Zacharia A, et al. Decay-accelerating factor attenuates remote ischemia-reperfusion-initiated organ damage. Clin Immunol. 2007; 124:311–327. [PubMed: 17631050]
14. Peckham RM, Handrigan MT, Bentley TB, et al. C5-blocking antibody reduces fluid requirements and improves responsiveness to fluid infusion in hemorrhagic shock managed with hypotensive resuscitation. J Appl Physiol. 2007; 102:673–680. [PubMed: 17068213]
15. Pfeifer R, Tarkin IS, Rocos B, et al. Patterns of mortality and causes of death in polytrauma patients-Has anything changed? Injury. 2009; 40:907–911. [PubMed: 19540488]
16. Szebeni J, Baranyi L, Savay S, et al. Complement activation during hemorrhagic shock and resuscitation in swine. Shock. 2003; 20:347–355. [PubMed: 14501949]
17. Ganter MT, Brohi K, Cohen MJ, et al. Role of the alternative pathway in the early complement activation following major trauma. Shock. 2007; 28:29–34. [PubMed: 17510601]
18. Wang Y, Li Y, Dalle Lucca SL, et al. Decay accelerating factor (CD55) protects neuronal cells from chemical hypoxia-induced injury. J Neuroinflammation. 2010; 7:24–36. [PubMed: 20380727]
19. Hecke F, Schmidt U, Kola A, et al. Circulating complement proteins in multiple trauma patients--correlation with injury severity, development of sepsis, and outcome. Crit Care Med. 1997; 25:2015–2024. [PubMed: 9403752]
20. Lublin DM, Atkinson JP. Decay-accelerating factor: biochemistry, molecular biology and function. Annu Immunol. 1989; 7:35–38.
21. Shenoy-Scaria AM, Kwong J, Fujita T, et al. Signal transduction through decay-accelerating factor. Interaction of glycosyl-phosphatidylinositol anchor and protein tyrosine kinase p56lck and p59fyn 1. J immunol. 1992; 149:3535–3541. [PubMed: 1385527]
22. Salter MW, Kalia LV. Src kinases: a hub for NMDA receptor regulation. Nat Rev Neurosci. 2004; 5:317–28. [PubMed: 15034556]
23. Okamoto K, Wang W, Rounds J, et al. Sublytic complement attack increases intracellular sodium in rat skeletal muscle. J Surg Res. 2000; 90:174–182. [PubMed: 10792960]
24. Xie Z, Cai T. Na+-K+--ATPase-mediated signal transduction: from protein interaction to cellular function. Mol Interv. 2003; 3:157–168. [PubMed: 14993422]
25. Zhang X, Kimura Y, Fang C, et al. Regulation of Toll-like receptor-mediated inflammatory response by complement in vivo. Blood. 2007; 110:228–236. [PubMed: 17363730]

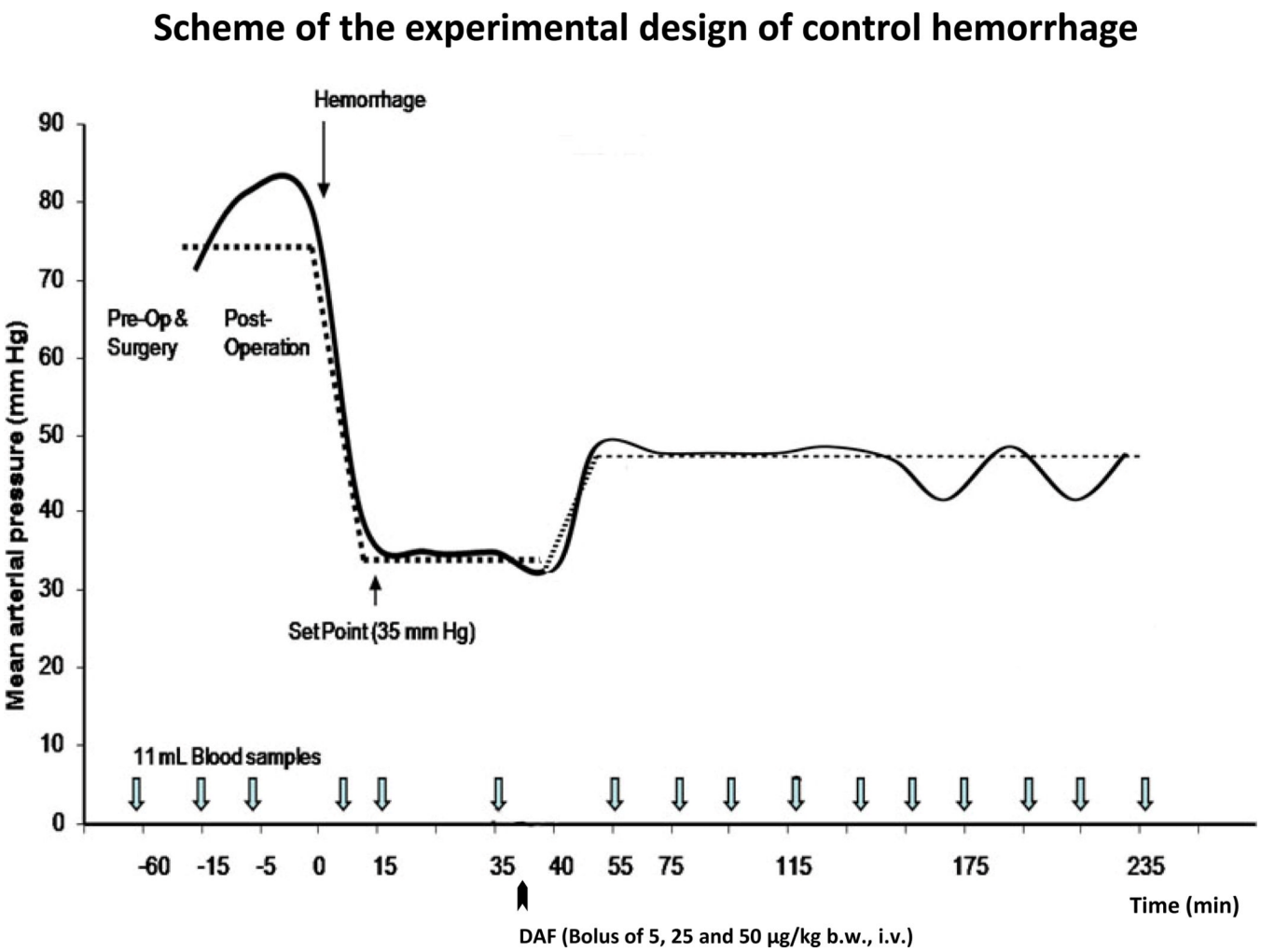


**Figure 1. Scheme of the experimental design**

Actual, target mean arterial blood pressure (MAP) and blood sample collection are shown. Recombinant human Decay-Accelerating Factor (DAF) was given as a bolus in 60 ml of PBS. Solid line actual and target mean arterial blood pressure, dashed line represents the proposed model mean arterial blood pressure.

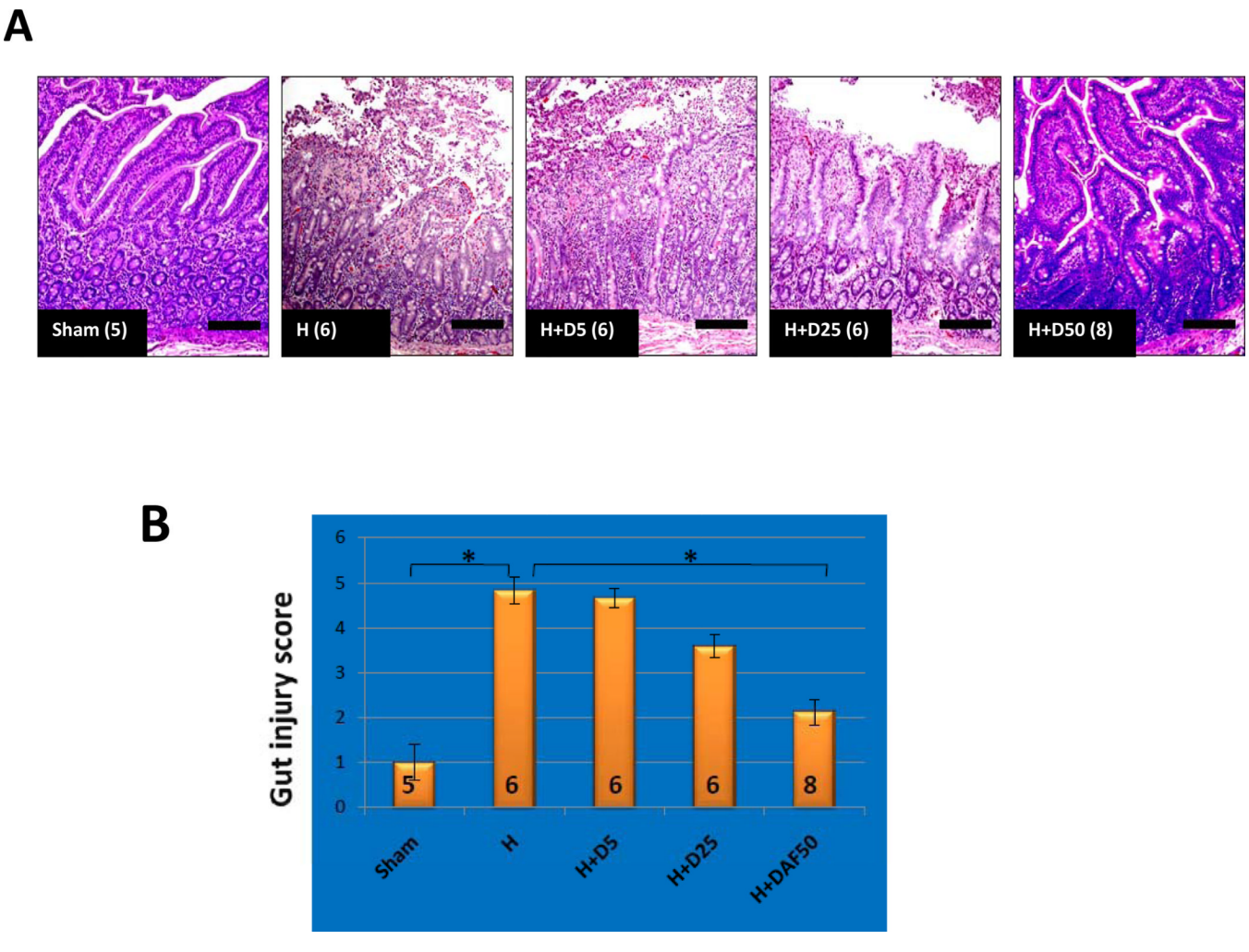


**Figure 2. DAF treatment attenuates hemorrhage-mediated intestinal injury of pigs**

(A) Representative histopathological changes of the small intestines are shown. Original magnification ×100. Scale bars = 50 μm. (B) Mucosal damage of small intestine was graded on a six-tiered scale (y-axis): 0 for normal villus; 1 for villi with tip distortion; 2 for villi lacking goblet cells and containing Guggenheims' spaces; 3 for villi with patch disruption of the epithelial cells: 4 for villi with exposed but intact lamina propria and epithelial cell sloughing; 5 for villi in which the lamina propria was exuding; and 6 for hemorrhaged or denuded villi. Group data were expressed as mean ± SEM and compared using one-way ANOVA followed by Tukey's Multiple Comparison Test with p values of < 0.05 considered significant. *$p$<0.05.

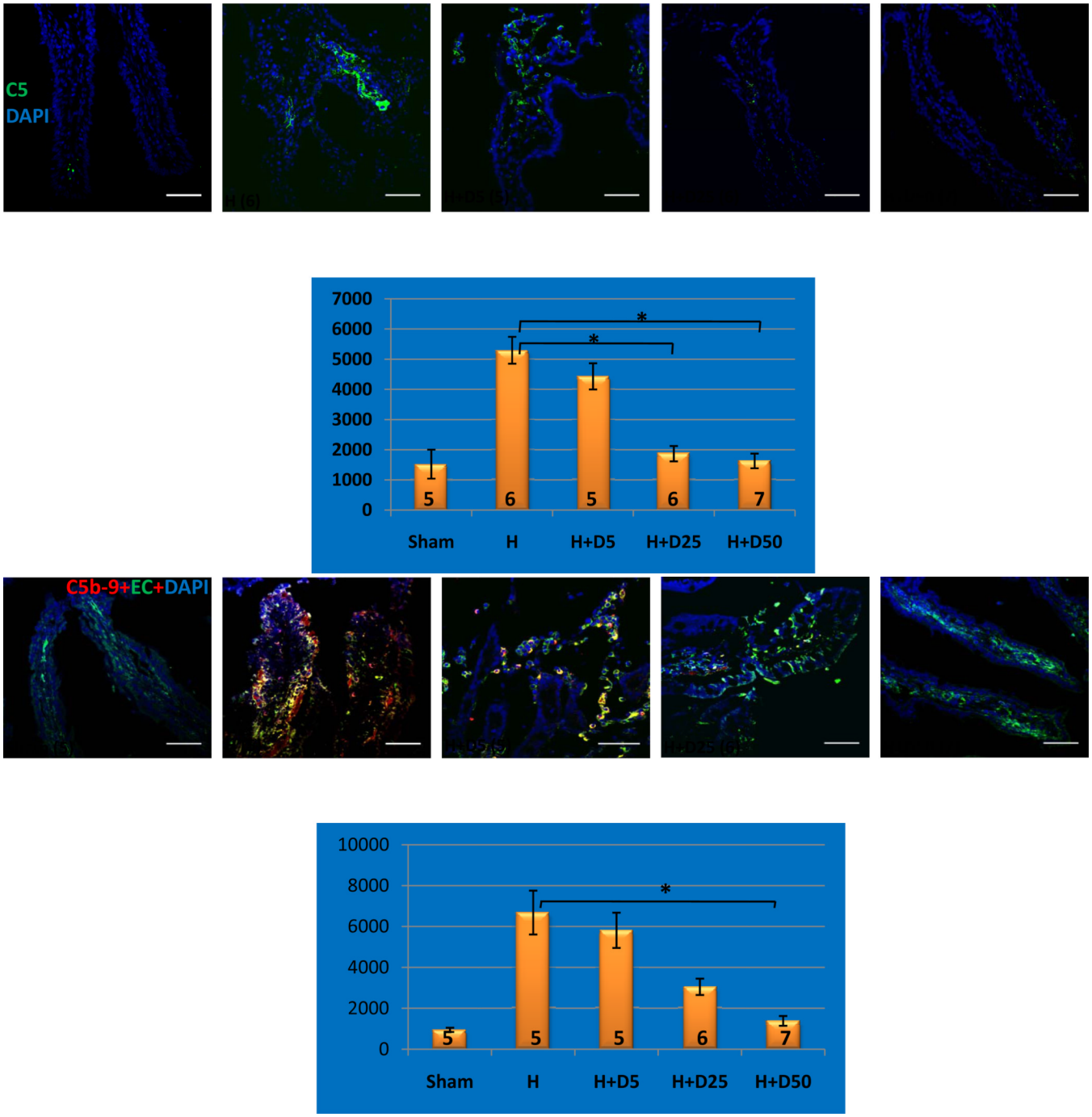


**Figure 3. DAF treatment decreases complement deposition and activation in small intestine tissue from hemorrhaged animals**

Representative confocal images of C5 deposition (A, top) and C5b-9 formation (B, top) in small intestine tissue detected by immunohistochemistry. The total fluorescent quantification of C5 deposition (A, bottom) and C5b-9 formation (B, bottom) in small intestine was evaluated by averaging the total area of fluorescence per slide to yield the average area of fluorescent deposit (y-axis) per group. Original magnification ×400. Scale bars in the pictures, 50μm. Group data are expressed as mean ± SEM and compared using

one-way ANOVA followed by Tukey's Multiple Comparison Test with p values of $< 0.05$ considered significant. $*p<0.05$.

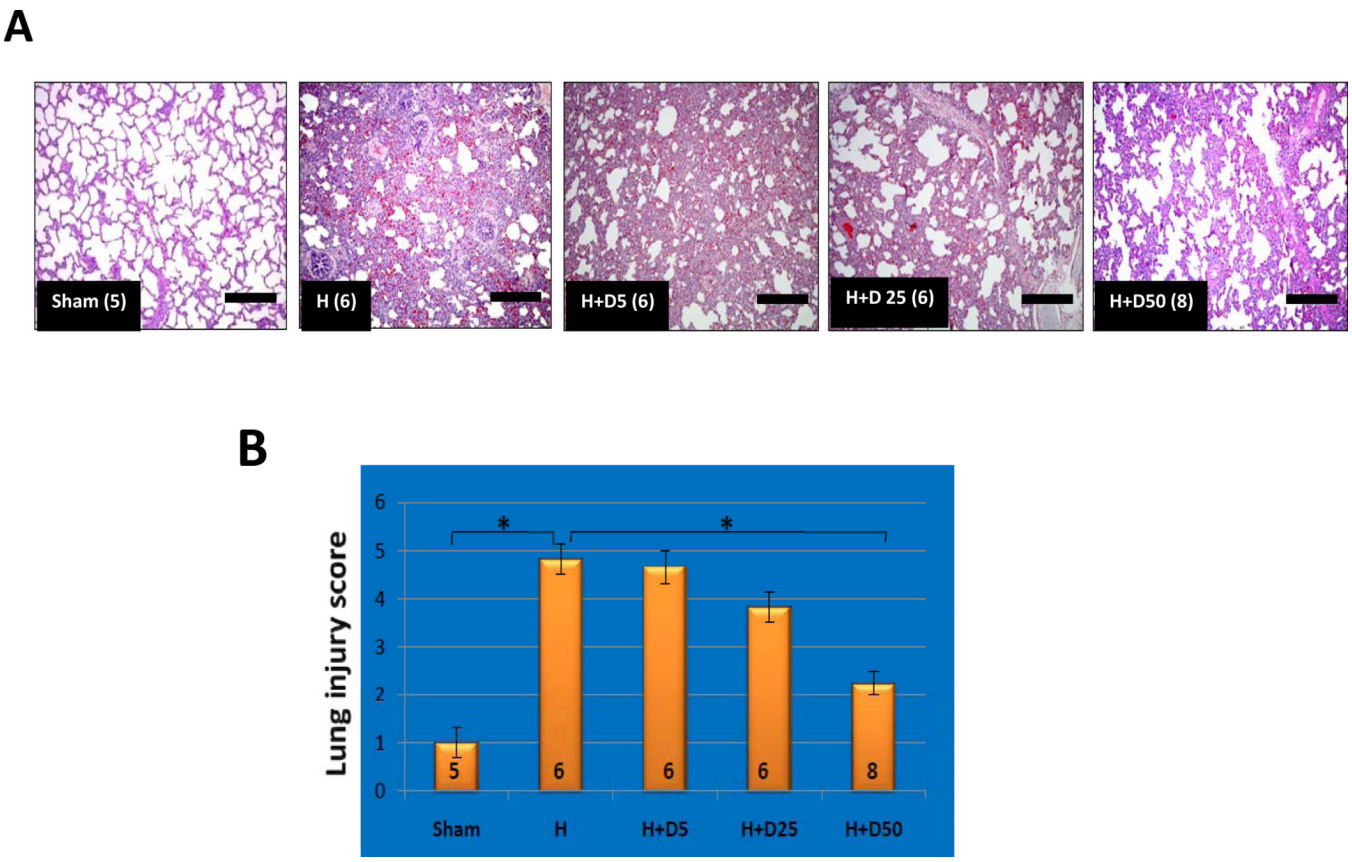


**Figure 4. DAF treatment mitigates lung injury in a swine hemorrhagic model**

(A) Representative histological microphotos (H&E staining) of the lungs. Original magnification ×100. Scale bars = 50 μm. (B) Lung injury scores were calculated using four parameters (alveolar fibrin edema, alveolar hemorrhage, septal thickening, and intra-alveolar inflammatory cells) as scored for: 1) severity (0: absent; 1, 2, and 3 for more severe changes) and 2) extent of injury (0: absent; 1: <25%; 2: 25–50%; 3: >50%). Total injury score (y-axis) for each slide was calculated as the sum of the extent plus the severity of injury. Group data were expressed as mean ± SEM and compared using one-way ANOVA followed by Tukey's Multiple Comparison Test with p values of < 0.05 considered significant. *$p$<0.05.

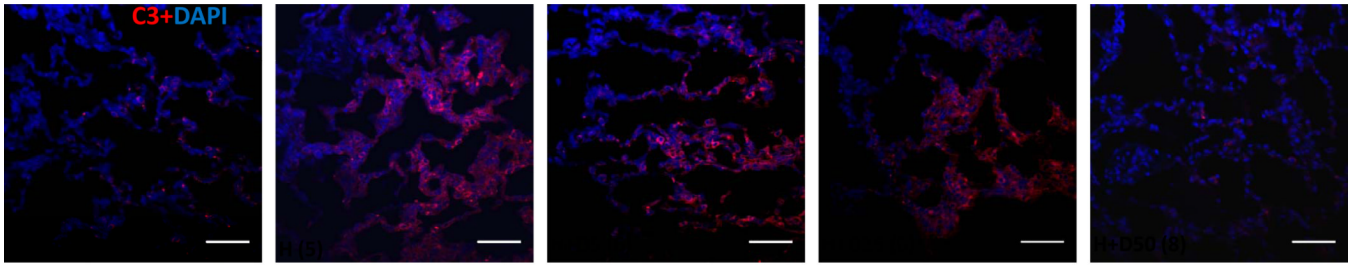


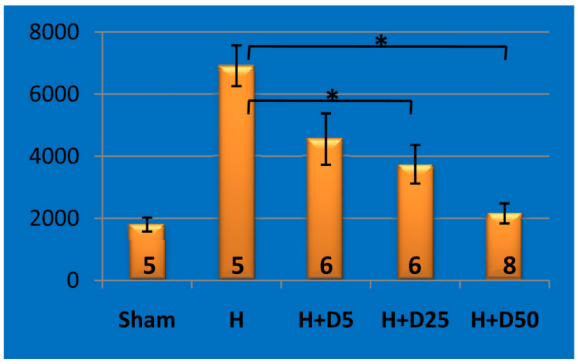


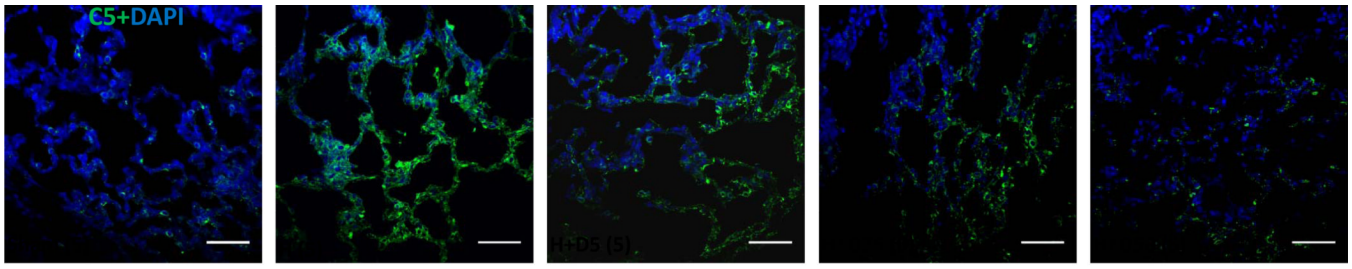


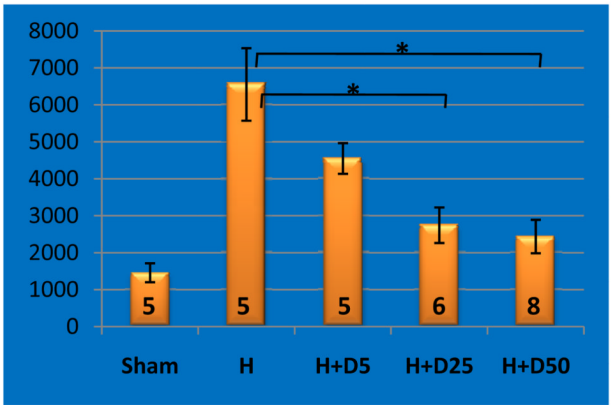

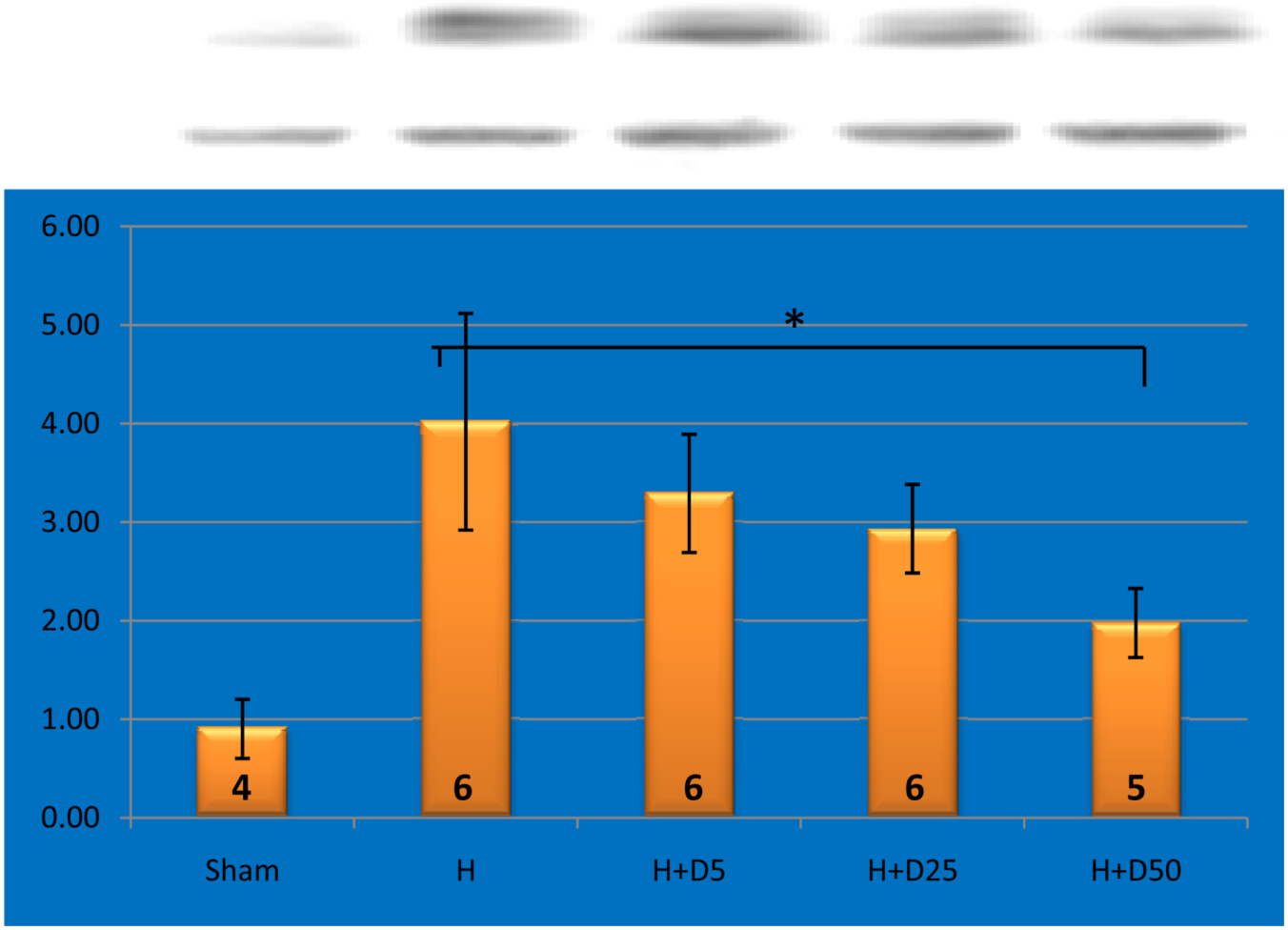


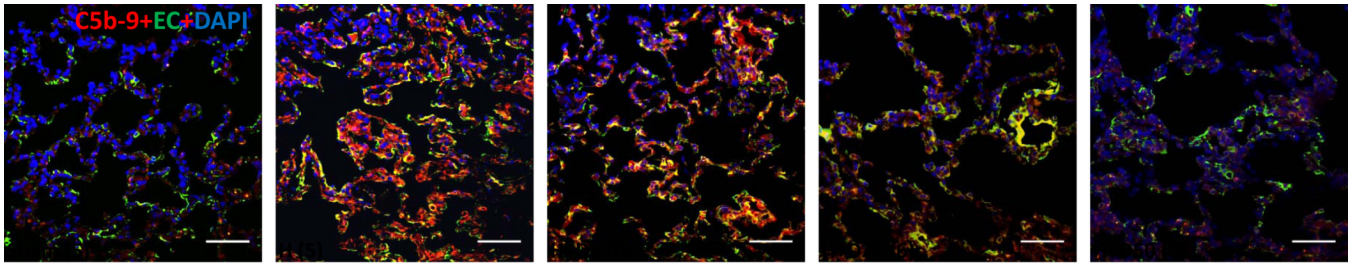


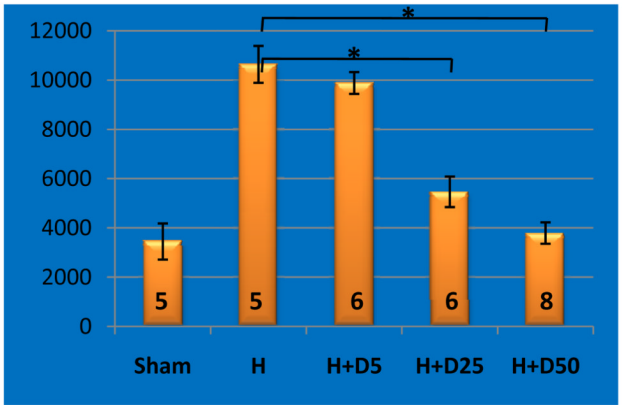

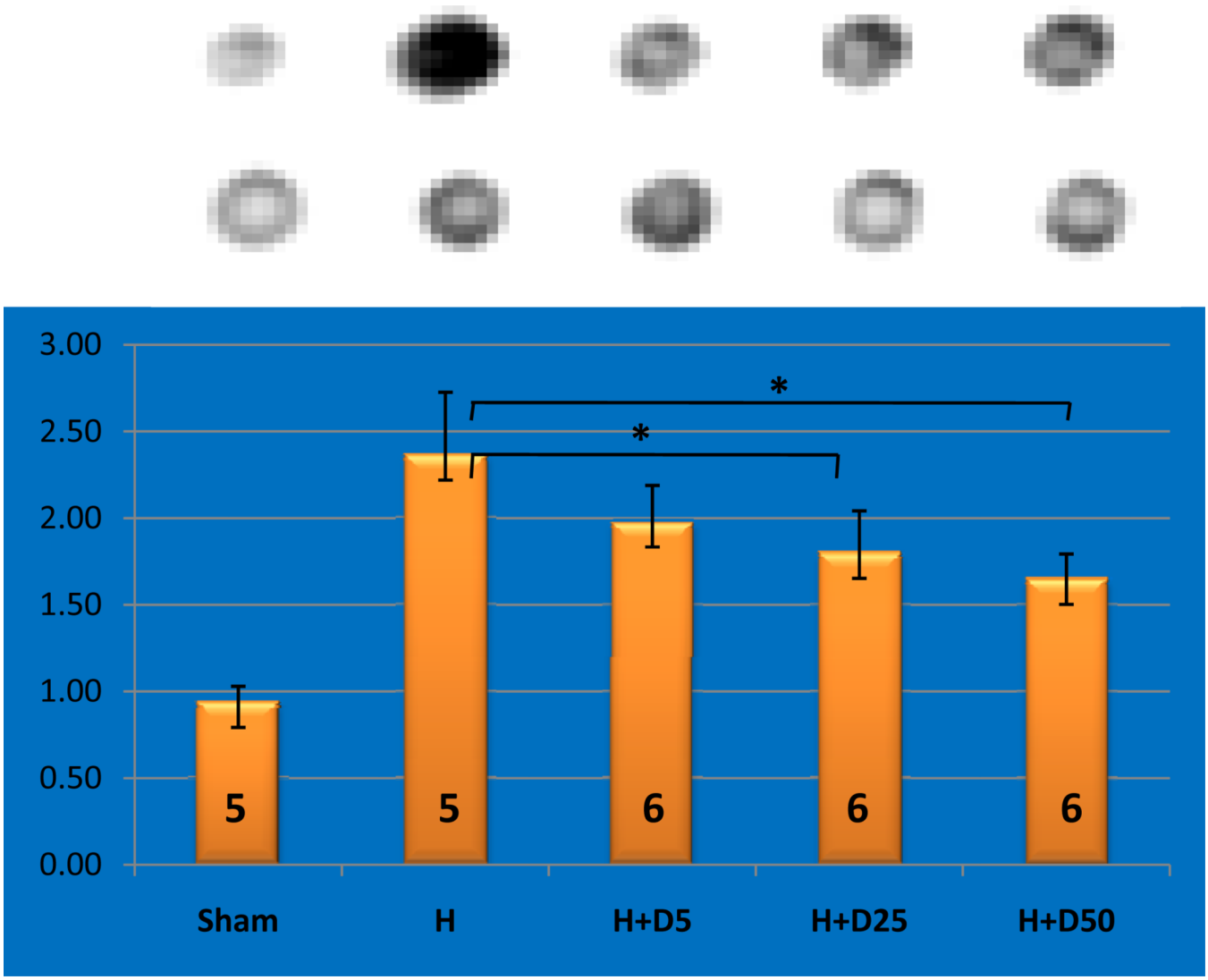


**Figure 5. DAF treatment reduces complement deposition and activation in lung tissue from hemorrhaged animals**

Representative immunohistochemical images of C3 deposition (A, top), C5 deposition (B, top), and C5b-9 formation (D, top) in the lung tissues. The total fluorescent quantification of C3 deposition (A, bottom), C5 deposition (B, bottom), and C5b-9 formation (D, bottom) in small intestine was evaluated by averaging the total area of fluorescence per slide to yield the average area of fluorescence deposit (y-axis) per group. Original magnification ×400. Scale bars in the pictures, 50μm. Local complement C3a generation by Western-blot (C, top) and C5b-9 formation by Dot-blot (E, top) were determined. The density (y-axis) of C3a (C, bottom) and C5b-9 (E, bottom) was measured using QuantityOne Software. Group data were expressed as mean ± SEM and compared using one-way ANOVA followed by Tukey's Multiple Comparison Test with p values of < 0.05 considered significant. *$p$<0.05.

**Table 1**

Pre- and posthemorrhage hemodynamic data

| | Group | | | | | |
|---|---|---|---|---|---|---|
| | **Sham** | **H** | **H+D5** | **H+D25** | **H+D50** | ***p* value** |
| **n** | **4–5** | **5–6** | **5–6** | **4–6** | **7–8** | |
| Body weight (kg) | 34.34±1.99 | 33.55±0.56 | 35.32±0.56 | 35.3±1.29 | 31.9±0.51 | ns |
| Shed blood (ml/kg) | | 25.69±3.22 | 23.3±3.1 | 26.16±1.27 | 23.97±2.33 | ns |
| Prehemorrhage MAP (mmHg) | 71.01±4.03 | 84.02±5.72 | 82.68±3.56 | 76.68±7.7 | 76.06±4.06 | ns |
| Postshock MAP (mmHg) | 82.1±3.03 | 36.26±0.35* | 36.36±0.07* | 35.06±0.87* | 35.39±1.14* | s |
| Final MAP (mmHg) | 54.08±3.61 | 35.77±2.8* | 37.9±3.54 | 36.37±6.32 | 42.5±3.17 | s |
| Prehemorrhage SI | 0.88±0.24 | 0.9±0.05 | 0.91±0.06 | 0.98±0.09 | 0.95±0.25 | ns |
| Postshock SI | 1.34±0.12 | 2.34±0.27* | 2.71±0.37* | 2.89±0.14* | 2.4±0.2* | s |
| Final SI | 1.03±0.07 | 3.61±0.49* | 3.54±0.38* | ≠4.07±0.58* | 3.06±0.0.29* | s |
| Prehemorrhage PP (mmHg) | 46.49±2.2 | 40.03±2.13 | 42.28±1.87 | 41.81±2.41 | 41.26±1.35 | ns |
| Postshock PP (mmHg) | 40.88±6.86 | 16.01±1.46* | 19.22±2.53* | 19.15±1.25* | 18.46±1.11* | s |
| Final PP (mmHg) | 38.73±3.4 | 15.44±2.63* | 19.79±2.6* | 18.12±2.26* | 18.49±2.14* | s |

Data are expressed as mean±SEM; n, number of animals; MAP, mean arterial blood pressure; SI, shock index is defined as the ration of heart rate to systolic blood pressure; PP, pulse pressure; ns, not significant; H, hemorrhage; D, DAF. Group data were compared using one-way ANOVA with Bonferonni post test.

*p<0.05 vs. sham;

≠p<0.05 vs. H+D50.

**Table 2**

pre- and posthemorrhage metabolic data

| | Group | | | | | |
|---|---|---|---|---|---|---|
| | **Sham** | **H** | **H+D5** | **H+D25** | **H+D50** | ***p* value** |
| **n** | **4–5** | **5–6** | **5–6** | **4–6** | **7–8** | |
| Prehemorrhage pH | 7.44±0.01 | 7.43±0.02 | 7.39±0.02 | 7.38±0.01 | 7.43±0.02 | ns |
| Postshock pH | 7.44±0.01 | 7.39±0.02 | 7.35±0.03 | 7.34±0.02 | 7.36±0.02 | ns |
| Final pH | 7.46±0.03 | 7.45±0.03 | 7.39±0.02 | 7.40±0.04 | 7.43±0.01 | ns |
| Prehemorrhage pO2 (mmHg) | 64.1±4.56 | 82.75±3.36 | 82.67±3.13 | 77.67±2.64 | 101.38±24.74 | ns |
| Postshock pO2 (mmHg) | 67.2±4.2 | 79.67±5.01 | 81.83±5.9 | 75.08±2.29 | 69.13±4.14 | ns |
| Final pO2 (mmHg) | 69.75±7.24 | 89.7±7.27 | 79.2±5.24 | 83.75±6.95 | 76.14±4.44 | ns |
| Prehemorrhage sO2 (%) | 91.60±1.72 | 95.92±0.71 | 95.33±0.83 | 94.67±0.48 | 95.69±1.0 | ns |
| Postshock sO2 (%) | 92.60±1.56 | 94.83±0.91 | 94.33±1.34 | 93.58±0.56 | 91.06±1.83 | ns |
| Final sO2 (%) | 93.50±1.58 | 96.8±0.86 | 94.9±1.09 | 95.13±1.76 | 94.64±1.07 | ns |
| Prehemorrhage pCO2 (mmHg) | 48.68±1.51 | 46.95±2.76 | 50.11±2.01 | 51.13±1.11 | 49.63±2.44 | ns |
| Postshock pCO2 (mmHg) | 48.39±0.95 | 46.65±1.74 | 50.47±1.73 | 53.07±2.45 | 56.56±2.67† | s |
| Final pCO2 (mmHg) | 47.96±3.27 | 41.96±4.04 | 50.19±4.49 | 48.2±5.4 | 49.96±2.25 | ns |
| Prehemorrhage base excess (mM) | 34.6±0.66 | 32.17±0.8 | 31.5±0.82 | 31.92±0.56 | 34.44±0.77 | ns |
| Postshock base excess (mM) | 34.5±0.5 | 29.42±1.47* | ≠29.25±0.75* | 30.25±0.67* | 33.31±0.82† | s |
| Final base excess (mM) | 35.25±0.66 | 30.10±1.38* | 31.9±1.95 | 30.63±1.59* | 34.29±1.11† | s |
| Prehemorrhage bicarbonate (mM) | 33.03±0.59 | 30.73±0.82 | 29.99±0.83 | 30.38±0.5 | 32.98±0.75 | ns |
| Postshock bicarbonate (mM) | 33.13±0.48 | 28.09±1.39* | ≠27.79±1.18* | ≠28.65±0.65* | 31.72±0.8† | s |
| Final bicarbonate (mM) | 33.86±0.64 | 28.94±1.32* | 30.33±1.82 | 29.29±1.45* | 32.92±1.06† | s |
| Prehemorrhage glucose (mg/dl) | 92.6±4.87 | 97±8.0 | 104.33±8.74 | 97.5±6.83 | 94±12.28 | ns |
| Postshock glucose (mg/dl) | 95.2±5.09 | 151±17.02 | ≠170.5±26.18* | 159±10.64* | 115.38±15.89 | s |
| Final glucose (mg/dl) | 110±14.4 | 88.4±22.62 | 145±20.97 | ≠157±27.82† | 92±23.76 | s |
| Prehemorrhage lactate (mM) | 0.9±0.17 | 1.14±0.13 | 1.45±0.18 | 1.69±0.11 | 0.74±0.05 | ns |
| Postshock lactate (mM) | 1.01±0.13 | 2.18±0.64 | 3.15±0.52* | 3.16±0.3* | 2.25±0.34 | s |
| Final lactate (mM) | 1.15±0.18 | 3.43±0.97* | 2.51±0.73 | 3.265±0.98 | 2.08±0.32 | s |

| | Group | | | | | |
|---|---|---|---|---|---|---|
| | **Sham** | **H** | **H+D5** | **H+D25** | **H+D50** | ***p* value** |
| **n** | **4–5** | **5–6** | **5–6** | **4–6** | **7–8** | |
| Prehemorrhage hemoglobin (g/dl) | 8.02±0.55 | 8.03±0.3 | 8.25±0.27 | 7.93±0.36 | 8.74±0.18 | ns |
| Postshock hemoglobin (g/dl) | 8.04±0.52 | 7.48±0.24 | 7.37±0.27 | 7.3±0.23 | 7.96±0.16 | ns |
| Final hemoglobin (g/dl) | 7.65±0.58 | 8.56±0.42 | 8.64±0.28 | 8.3±0.41 | 8.4±0.28 | ns |
| Prehemorrhage hematocrit (%) | 23.6±1.6 | 23.67±0.88 | 24.33±0.8 | 23.3±1.09 | 25.75±0.53 | ns |
| Postshock hematocrit (%) | 23.6±1.54 | 22±0.68 | 21.67±0.8 | 21.5±0.67 | 23.38±0.46 | ns |
| Final hematocrit (%) | 22.5±1.71 | 25.2±1.24 | 25.4±1.14 | 24.5±1.19 | 24.71±0.84 | ns |
| Prehemorrhage potassium ( mM) | 3.84±0.27 | 4.02±0.31 | 4.13±0.24 | 4.05±0.19 | 3.91±0.31 | ns |
| End of hemorrhage potassium (mM) | 4.06±0.22 | 4.95±0.86* | 4.733±0.41 | 4.67±0.32 | 4.6±0.22 | s |
| Final potassium (mM) | 4.15±0.24 | 6.48±0.88* | ‡^6.12±0.7* | 7.1±0.64* | †5.4±0.52* | s |
| Prehemorrhage $Na^+$ (mM) | 134±0.71 | 134.33±0.88 | 135.33±0.92 | 134.33±0.49 | 134.38±0.68 | ns |
| Postshock $Na^+$ (mM) | 133.4±0.68 | 132.83±0.87 | 133.67±1.2 | 133.33±0.62 | 133.50±0.62 | ns |
| Final $Na^+$ (mM) | 131.75±0.86 | 130.8±1.16 | 131.4±1.5 | 130.5±1.26 | 131.86±0.55 | ns |
| Prehemorrhage $iCa^{2+}$(mM) | 1.19±0.04 | 1.32±0.02 | ‡1.44±0.02* | ‡1.41±0.02* | 1.24±0.01 | s |
| Postshock $iCa^{2+}$ (mM) | 1.18±0.05 | 1.29±0.02 | ‡1.38±0.02* | ‡1.38±0.02* | 1.2±0.02 | s |
| Final $iCa^{2+}$ (mM) | 1.08±0.06 | 1.21±0.03 | ‡†1.36±0.02* | ‡1.35±0.02* | 1.11±0.04 | s |

Data are expressed as mean±SEM; n, number of animals; ns, not significant; H, hemorrhage; D, DAF. Group data were compared using one-way ANOVA with Bonferonni post test.

*p<0.05 vs. sham;

†p<0.05 vs. H;

‡p<0.05 vs. H+D50.

Data are expressed as mean±SEM; n, number of animals; ns, not significant; H, hemorrhage; D, DAF. Group data were compared using one-way ANOVA with Bonferonni post test.

*p<0.05 vs. sham;

†p<0.05 vs. H;

‡p<0.05 vs. H+D25;

^p<0.05 vs. H+D50.